Progress in Fractional Differentiation and Applications
An International Journal

http://dx.doi.org/10.18576/pfda/120206

Investigation of Lung Cancer by Early Detection and Anticancer Cell's Measures with Control Strategies Utilizing Mathematical Modeling Approach

Muhammad Farman[1,2,*], *Aqeel Ahmad*[1,3], *Khurram Faiz*[3], *Aseel Smerat*[4,5], *Muhammad Manan Akram* [6], *and Mohamed Hafez*[7,8]

[1] Mathematics Research Center, Department of Mathematics, Near East University, 99138 Nicosia, Turkey
[2] International Center for Interdisciplinary Research in Sciences, The University of Lahore, Lahore, Pakistan
[3] Department of Mathematics, Ghazi University D G Khan 32200, Pakistan
[4] Faculty of Educational Sciences, Al-Ahliyya Amman University, Amman 19328, Jordan
[5] Department of Biosciences, Saveetha School of Engineering, Saveetha Institute of Medical and Technical Sciences, Chennai, 602105, India
[6] Washington University of Science and Technology, Washington, USA
[7] Faculty of Engineering and Quantity Surviving, INTI International University Colleges, Nilai, Malaysia
[8] Faculty of Mangement, Shinawatra, Pathum Thani, Thailand

Received: 2 Jan. 2026, Revised: 18 Feb. 2026, Accepted: 20 Mar. 2026
Published online: 1 Apr. 2026

Abstract: Lung cancer remains one of the most prevalent and life-threatening chronic respiratory diseases worldwide, demanding effective diagnostic and therapeutic strategies. In this study, we propose a novel deterministic mathematical model, denoted as TCDIL_2, to investigate the impact of IL_2 cytokine therapy on the immune system's anticancer response. The model is structured into four epidemiological compartments and is analyzed through both qualitative and quantitative approaches. Local stability analysis is performed under limited data conditions, while equilibrium points, the basic reproduction number (R_0), and sensitivity indices are systematically examined. The next-generation method is employed to compute R_0, offering insight into disease progression across compartments, whereas sensitivity analysis highlights the influence of key parameters on system dynamics. Global stability is assessed via Lyapunov functions, establishing conditions under which IL_2 therapy benefits immunocompromised individuals. For numerical simulations, a nonstandard finite difference (NSFD) scheme based on an implicit method is developed and benchmarked against Euler's method and the fourth-order Runge–Kutta scheme, ensuring improved accuracy. Simulations conducted in MATLAB illustrate disease trajectories for both early- and mid-stage detection and evaluate the effectiveness of immune-based interventions. The results enhance understanding of cancer dynamics, provide public health perspectives on immunotherapy outcomes, and contribute to evidence-based strategies for controlling cancer.

Keywords: Mathematical Modeling; Stability analysis; Reproductive number; Sensitivity analysis; Non-standard finite difference (NSFD).

1 Introduction

The integration of mathematics and biology can be traced back to the 13th century, when Leonardo Fibonacci introduced the Fibonacci sequence, which significantly impacted population studies. Over time, mathematicians like Bernoulli and others applied mathematical principles to describe the forms of microorganisms. This eventually led to Wilhelm Reinke being the first to define "biomathematics" in 1901. This interdisciplinary field employs mathematical models to explore and understand the fundamental mechanisms governing the structure and behavior of biological systems. In recent decades, biological sciences have seen remarkable advancements, largely driven by technological progress, a trend that is expected to continue [1]. Mathematical modeling has played a crucial role in this growth, helping to reveal the

* Corresponding author e-mail: farmanlink@gmail.com

complexities of biological processes. With the development of modern computer algebra systems, the handling of complex mathematical systems has become more efficient, allowing researchers to focus more on the field of mathematical biology rather than on solving intricate techniques [2].

Cancer is a disease that can originate in almost any part of the human body. The genome is crucial for the growth and division of human cells, which create tissues and organs such as the liver, heart, and lungs. However, disruptions in gene regulation can lead to uncontrolled cell growth, resulting in the formation of tumors. According to data from the Canadian Cancer Society, an estimated 31,000 men and 26,000 women were expected to die from cancer in Canada in 2015. Cancer encompasses a broad spectrum of conditions, with more than 200 distinct diseases falling under its category. It remains a complex and challenging field, driving ongoing research to understand the intricate interactions between tumor cells and the immune system. Researchers employ various methodologies, including mathematical modeling, to study these interactions [3,4,5]. Ordinary differential equations are particularly useful in this context, as they help elucidate the dynamics between tumors and the immune system. This approach provides insights into how immune cells respond to the spread of cancer cells [6,7,8]. Additionally, fractional-order differential equations offer enhanced modeling capabilities compared to traditional derivatives such as [9,10,11,12], leading to a deeper understanding of cancer dynamics.

According to the American Cancer Society, lung cancer is the most frequent cancer in both men and women and the main cause of cancer-related deaths. People who smoke are more likely to develop lung cancer because it starts in the lungs. Wheezing, blood in the cough, chest discomfort, and weight loss are typical symptoms. Recent years have seen a decrease in death rates due to less smoking, improved identification, and improved treatment. In Figure 1, comparison of healthy lung and lung cancer are illustrated.

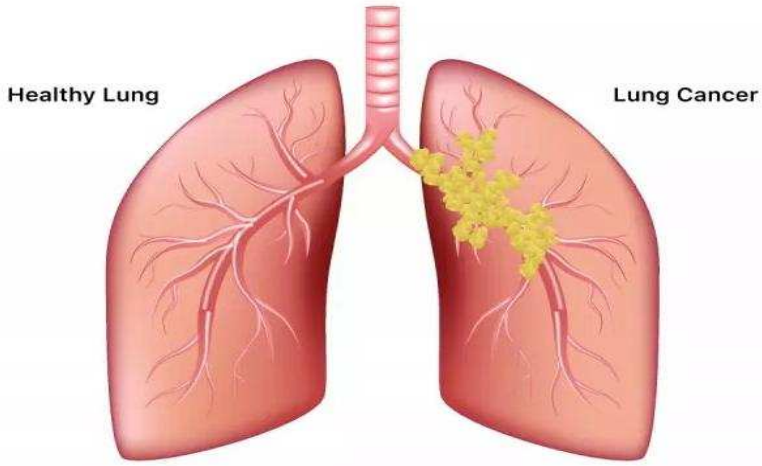

Fig. 1: Lung cancer symptoms.

Several studies have provided unique mathematical models that clarify the complex relationships between tumors and the immune system, illuminating important immunological elements and therapeutic approaches [13]. Trisilowati et al. created a mathematical model that concentrated on patient therapy utilizing dendritic cells, where natural killer cells with immunological elements [14,15]. Kirschner and Tsygvintsev described a novel tumor treatment method along with a mathematical model predicting the immune system's reaction to cancers [16,17]. Comprehensive reviews and perspectives have also made a substantial contribution to our comprehension of cancer immunotherapy [19], emphasizing the role of T lymphocyte regulation and addressing various clinical trials and related side effects [20] furnished into systemic immunity in cancer treatment. More computational models have investigated the influence of particular elements on tumor behavior. Scientists created a model to show how different tumor features and treatment approaches affect outcomes [21,22]. Researchers Philip and Schietinger emphasized open research questions and investigated variables affecting T cells' receptivity to immunotherapy [23]. Clinical settings have been the focus of research on predictive modeling and patient selection optimization. A multi-modality technique was employed by Casiraghi et al. [24] to determine prognostic variables for patient selection, whereas Liang et al. and Chao et al. investigations focused on developing prediction nomograms and algorithms, respectively [25,26]. In a retrospective analysis, Li et al. [27] looked at complicated EGFR mutations in NSCLC patients. Decker et al. also conducted a

thorough literature review [18] on immunotherapy's acceptability and model system development, noting possible advances in tumor treatment approaches [33,34,35,36].

The theory of weakly nonlinear wave propagation in superposed fluids with magnetic fields present is examined by the author [37]. Investigating the dynamic features of the generalized equation controlling shallow water waves in (3+1) dimensions is the aim of the author [38]. Some instabilities observed in modulated wave-trains are driven by the modified unstable nonlinear Schrödinger equation, which also describes the temporal evolution of disturbances in marginally stable or unstable media [39]. The propagation of shocks and dust-ion-acoustic waves in evenly magnetized electron-positron-ion plasmas in three dimensions is studied by a different author [40]. The author intends to extend the application of the projected fractional improved Adomian Decomposition technique (fIADM) to the fractional order new coupled Korteweg-de Vries (cKdV) system [41].

Motivated by the implications highlighted above, this study delves into the dynamics of the deterministic mathematical model, TCDIL_2, focusing on early lung cancer detection and treatment. This model integrates IL_2 cytokine, bolstering the immune system's anticancer response. The article introduces a structured lung cancer model comprising four compartments. By determining basic characteristics such equilibria points, reproductve number, and stability and doing sensitivity analysis, we first confirm the model's validity. Subsequently, we examine global stability, particularly regarding individuals with compromised immunity due to IL_2 cytokine, employing Lyapunov functions for analysis. We then derive numerical solutions utilizing the Non-Standard Finite Difference (NSFD) scheme, comparing them with Euler's and RK4 methods to ensure accuracy. These results are further validated through simulations carried out using MATLAB. These results greatly advance our knowledge of the dynamics of disease transmission and direct the creation of successful control measures based on proven results.

The article is structured into eight sections. Section 2 details the model's development and description. Section 3 focuses on the qualitative analysis of the model, while Section 4 delves into the sensitivity analysis of the lung cancer model. Section 5 reports on the stability features of the considered model. Section 6 discusses the impact of global stability, and numerical solutions are derived using the Euler method, the Runge-Kutta method, and the Non-Standard Finite Difference (NSFD) Scheme. In Section 7, we present the simulation results. Lastly, Section 8 concludes by summarizing the major findings of this study.

2 Model Development

2.1 Description of the TCDIL_2 model

Understanding disease spread patterns and developing effective control strategies heavily relies on mathematical models of infectious diseases. Therefore, constructing these models requires a focus on outlining the disease's epidemiological characteristics and pinpointing crucial, adjustable parameters for disease control.

This section presents the formulation of a mathematical model for lung cancer treatment that incorporates the cytokine IL_2. Unlike the earlier TCD framework described in [28], the proposed model is denoted as TCDIL_2. In this framework, "T" refers to tumor cells, "C" to $CD8^+$ T cells, "D" to dendritic cells, and "IL_2" to the cytokine under consideration. The logistic growth of tumor cells is expressed by the term $\beta T(1-\gamma T)$. Tumor cell elimination is governed by two mechanisms: a constant rate δ due to dendritic cells and a rate ψ due to $CD8^+$ T cells. The parameter κ represents the natural death rate of $CD8^+$ T cells, while σ accounts for the generation of dendritic cells. The interaction between $CD8^+$ T cells and dendritic cells is captured by the rate ν, which describes the inactivation of dendritic cells. In addition, η denotes the natural death rate of dendritic cells. The cytokine IL_2 enters the system through a source term λ, which modulates the dendritic cell population, while d represents the natural death rate associated with IL_2.

Figure 2 depicts the flow diagram illustrating the newly developed TCDIL_2 model.

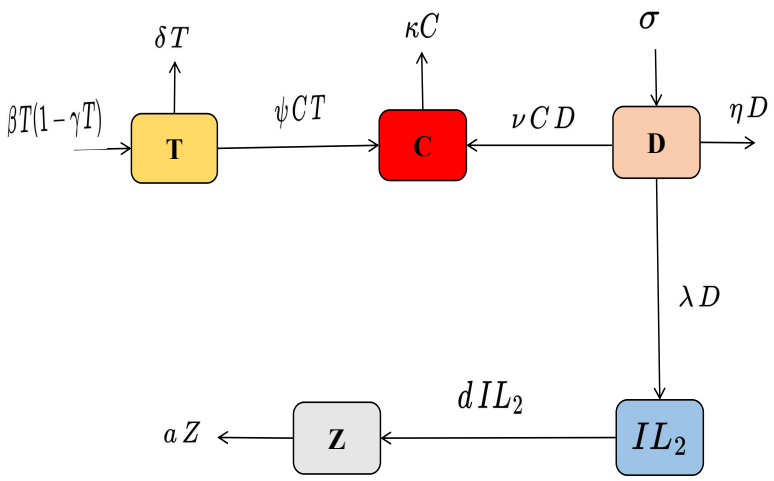

Fig. 2: Flowchart shows the developed model formulation.

Hence, the foundational model for lung cancer in the human population is outlined as follows:

$$\begin{aligned}
\frac{dT}{dt} &= \beta T(1-\gamma T) - \delta T - \psi CT,\\
\frac{dC}{dt} &= \psi CT + \nu CD - \kappa C,\\
\frac{dD}{dt} &= \sigma - \nu CD - \eta D - \lambda D,\\
\frac{dIL_2}{dt} &= \lambda D - dIL_2,
\end{aligned} \tag{1}$$

with initial conditions:

$$T(0) = T^0,\ C(0) = C^0,\ D(0) = D^0,\ IL_2(0) = IL_2^0.$$

3 Theoretical Insights into the Devised Model

The upcoming section will concentrate on the mathematical formulation encapsulated in model (1). Our analysis will delve into determining the equilibrium points and computing the fundamental reproduction number.

3.1 Analysis of equilibrium points

At these stable stages in the disease's course, the number of new infections equals the number of recoveries and deaths. This section describes how the suggested system's pandemic and disease-free equilibrium points were calculated. The equations connected with model (1) can be solved to find these equilibrium points: $\frac{dT}{dt} = \frac{dC}{dt} = \frac{dD}{dt} = \frac{dIL_2}{dt} = 0$.

Hence, the disease free equilibrium points are:

$$D_1(T, C, D, IL_2) = \left(0, 0, \frac{\sigma}{\lambda+\eta}, \frac{\lambda\sigma}{d(\lambda+\eta)}\right).$$

Furthermore, the endemic points of equilibrium are given as $D_2(T^*, C^*, D^*, IL_2^*)$.
where

$$
\begin{aligned}
T^* &= \frac{\psi^2\eta + \beta\nu\psi + \gamma\beta\kappa\nu + \lambda\psi^2 - \delta\nu\psi - \mathfrak{E}}{2\gamma\beta\nu\psi},\\
C^* &= -\frac{\gamma\beta\nu\kappa + \nu\delta\psi + \psi^2\lambda + \eta\psi^2 - \nu\beta\psi - \mathfrak{E}}{2\nu\psi^2},\\
D^* &= \frac{\nu\gamma\kappa\beta - \psi\beta\nu + \nu\delta\psi - \psi^2\lambda - \psi^2\eta + \mathfrak{E}}{2\gamma\beta\nu^2},\\
IL_2^* &= \frac{\lambda(\gamma\beta\nu\kappa - \nu\beta\psi + \delta\psi\nu - \psi^2\eta - \psi^2\lambda + \mathfrak{E})}{2d\gamma\beta\nu^2},
\end{aligned}
\tag{2}
$$

where $\mathfrak{E} = \sqrt{4\gamma\beta\sigma\nu^2\psi^2 + (\nu\beta(\psi - \gamma\kappa) + \psi(-\nu\delta + \psi(\eta + \lambda)))^2}$.

3.2 Reproductive number

One of the most important metrics for determining how contagious or transmissible an infectious disease is is the fundamental reproduction number, or R_0. It shows the typical number of people in a vulnerable demographic infected by a single infectious individual. R_0 biologically mimics the transmissibility and contagiousness of the disease. When $R_0 > 1$, the disease can continue to spread throughout the population and perhaps cause an outbreak. In contrast, if $R_0 < 1$, the infection may gradually vanish from the population since it is unlikely to start a self-sustaining spread chain.

The matrices F and V are evaluated at the disease-free equilibrium point D_1, where they represent the Jacobian matrices of the new infection terms and the transition terms, respectively. In this framework, the entry in the (i, j) position of F denotes the rate at which individuals in compartment j generate new infections in compartment i. Conversely, the (i, j) entry of V characterizes the transfer, progression, or removal of infection within compartment i. To determine the basic reproduction number, it is essential to compute the spectral radius of the matrix product FV^{-1} at the disease-free equilibrium.

$$J_0 = F - V. \tag{3}$$

Equation (1) is used in our constructed model to find the matrices F and V:

$$
F = \begin{pmatrix} \beta & 0 & 0 & 0 & 0 \\ 0 & \frac{\sigma\nu}{\mathfrak{A}} & 0 & 0 & 0 \\ 0 & -\frac{\sigma\nu}{\mathfrak{A}} & 0 & 0 & 0 \\ 0 & 0 & \lambda & 0 & 0 \end{pmatrix} \quad \textit{and} \quad V = \begin{pmatrix} \delta & 0 & 0 & 0 & 0 \\ 0 & \kappa & 0 & 0 & 0 \\ 0 & 0 & \mathfrak{A} & 0 & 0 \\ 0 & 0 & 0 & d & 0 \end{pmatrix},
$$

where $\mathfrak{A} = \lambda + \eta$.

$$
V^{-1} = \begin{pmatrix} \frac{1}{\delta} & 0 & 0 & 0 & 0 \\ 0 & \frac{1}{\kappa} & 0 & 0 & 0 \\ 0 & 0 & \frac{1}{\mathfrak{A}} & 0 & 0 \\ 0 & 0 & 0 & \frac{1}{d} & 0 \end{pmatrix}, \tag{4}
$$

$$K = FV^{-1}. \tag{5}$$

So,

$$
K = \begin{pmatrix} \frac{\beta}{\delta} & 0 & 0 & 0 & 0 \\ 0 & \frac{\sigma\nu}{\kappa(\mathfrak{A})} & 0 & 0 & 0 \\ 0 & -\frac{\sigma\nu}{\kappa(\mathfrak{A})} & 0 & 0 & 0 \\ 0 & 0 & \frac{\lambda}{\mathfrak{A}} & 0 & 0 \end{pmatrix}. \tag{6}
$$

Thus,

$$|K - \Lambda I| = 0.$$

$$
\begin{vmatrix} \frac{\beta}{\delta} - \Lambda & 0 & 0 & 0 & 0 \\ 0 & \frac{\sigma\nu}{\kappa(\mathfrak{A})} - \Lambda & 0 & 0 & 0 \\ 0 & -\frac{\sigma\nu}{\kappa(\mathfrak{A})} & -\Lambda & 0 & 0 \\ 0 & 0 & \frac{\lambda}{\mathfrak{A}} & -\Lambda & 0 \end{vmatrix} = 0. \tag{7}
$$

The following is the result of solving the determinant above: (Λ)

$$\Lambda = \frac{\beta}{\delta},$$
$$\Lambda = \frac{\sigma\nu}{\kappa(\mathfrak{A})}. \tag{8}$$

The Reproduction number R_0 may be stated as follows as it is the primary eigenvalue of the matrix FV^{-1}.

$$R_0 = \frac{\sigma\nu}{\kappa(\mathfrak{A})}. \tag{9}$$

Both R_0 are valid and are less than one under considered parameters but considered $R_0 = \frac{\sigma\nu}{\kappa(\mathfrak{A})}$ capture the maximum parameters and will be helpful in sensitivity analysis to capture the real impact rate of each parameter.

4 Sensitivity Analysis

Sensitivity analysis is crucial for determining the relative effects of several factors on a model's stability, especially in cases when the data is unclear. This analysis also helps identify the key factors in the system. We compute the normalized forward sensitivity indices for the parameters denoted by n with respect to R_0. Let's think about:

$$\Delta_n^{R_0} = \frac{\partial R_0}{\partial n}\frac{n}{R_0}.$$

The estimated sensitivities regarding the reproduction number for various parameters are provided as follows:

$$\begin{aligned}
\frac{\partial R_0}{\partial \sigma} &= \frac{\nu}{\kappa(\mathfrak{A})} &&< 0,\\
\frac{\partial R_0}{\partial \nu} &= \frac{\sigma}{\kappa(\mathfrak{A})} &&> 0,\\
\frac{\partial R_0}{\partial \kappa} &= -\frac{\sigma\nu}{\kappa^2(\mathfrak{A})} &&< 0,\\
\frac{\partial R_0}{\partial \lambda} &= -\frac{\sigma\nu}{\kappa(\mathfrak{A})^2} &&< 0,\\
\frac{\partial R_0}{\partial \eta} &= -\frac{\sigma\nu}{\kappa(\mathfrak{A})^2} &&< 0.
\end{aligned} \tag{10}$$

where $\mathfrak{A} = \lambda + \eta$.

One method that is frequently used to find factors that have a large influence on the reproduction number R_0 is sensitivity analysis. A relationship with R_0 that is directly proportional is shown by a positive value, whereas an inversely proportional relationship is indicated by a negative value. When we alter the parameters, we find that the value of R_0 is extremely sensitive. In our study, the parameters show growth for ν and contraction for σ, κ, λ, and η. Therefore, prophylaxis should come before therapy for effective infection control.

The sensitivity behavior of several parameters to the fundamental reproduction number R_0 is displayed in Figure 3-11.

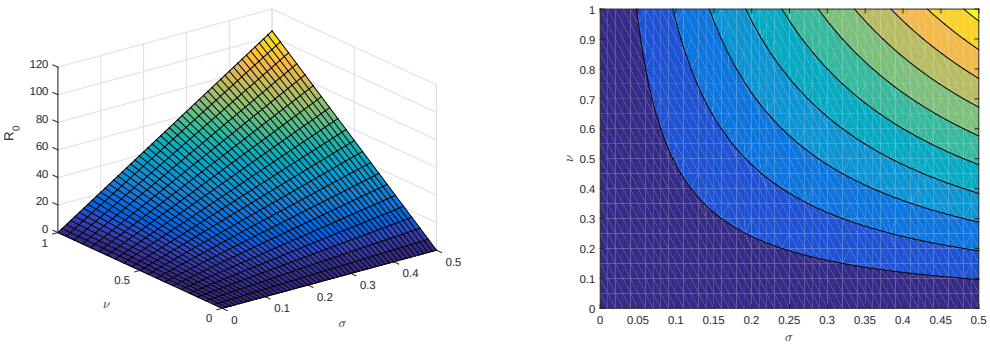

Fig. 3: R_0 and contour phase under parameter σ and ν

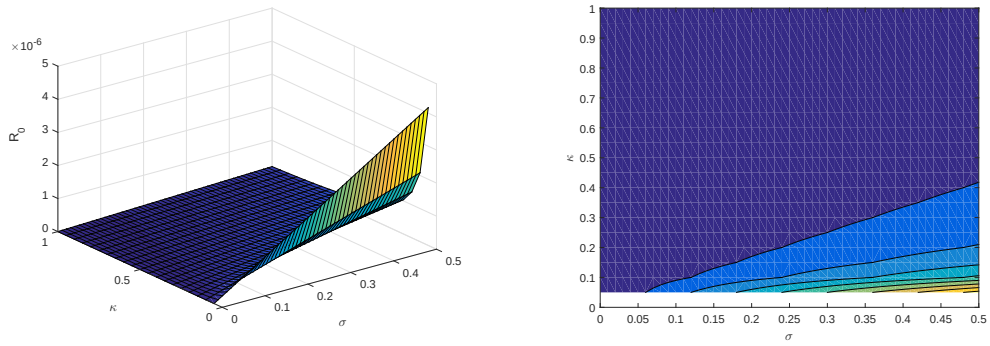

Fig. 4: R_0 and contour phase under parameter σ and κ

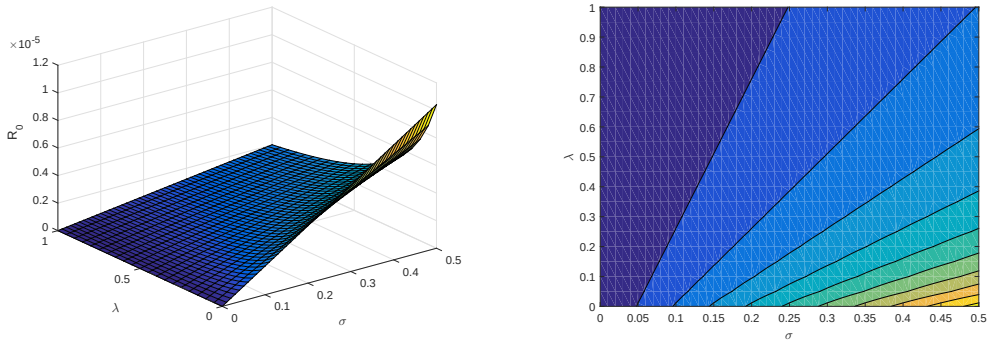

Fig. 5: R_0 and contour phase under parameter σ and λ

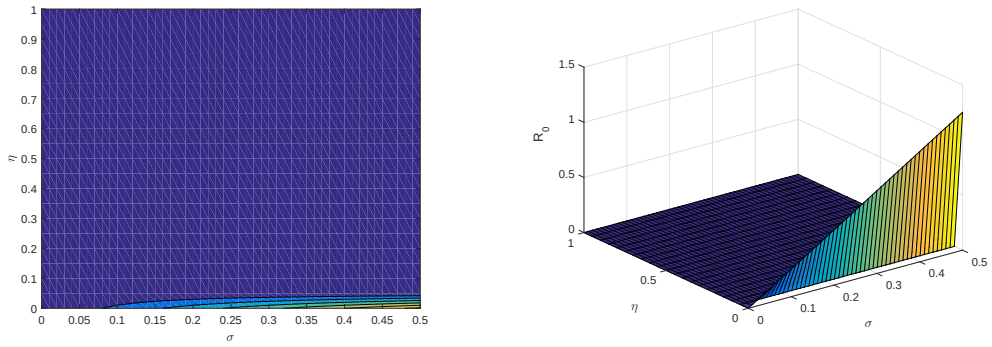

Fig. 6: R_0 and contour phase under parameter σ and η

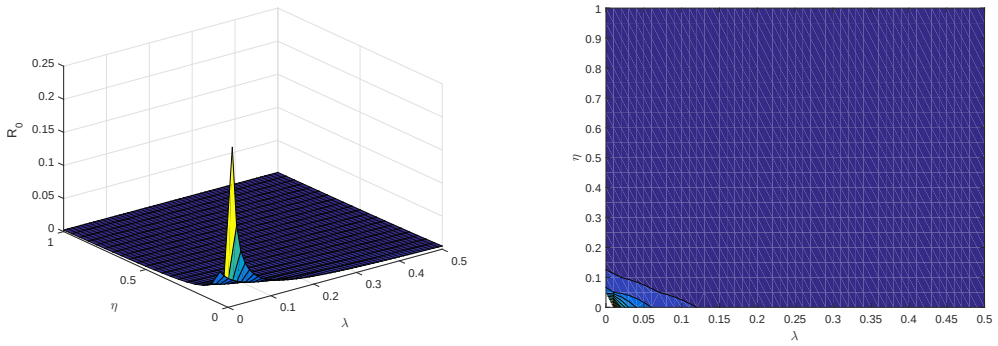

Fig. 7: R_0 and contour phase under parameter λ and η

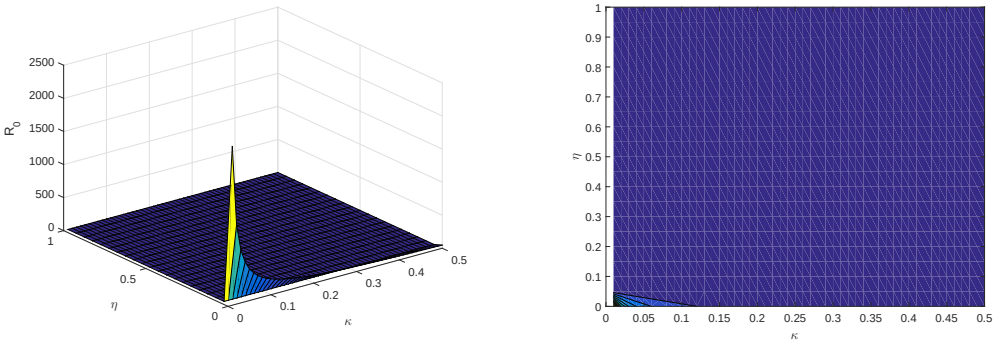

Fig. 8: R_0 and contour phase under parameter η and κ

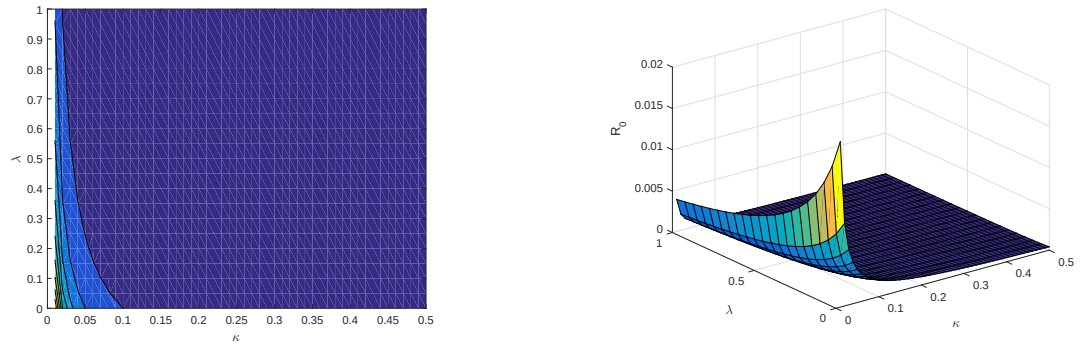

Fig. 9: R_0 and contour phase under parameter κ and λ

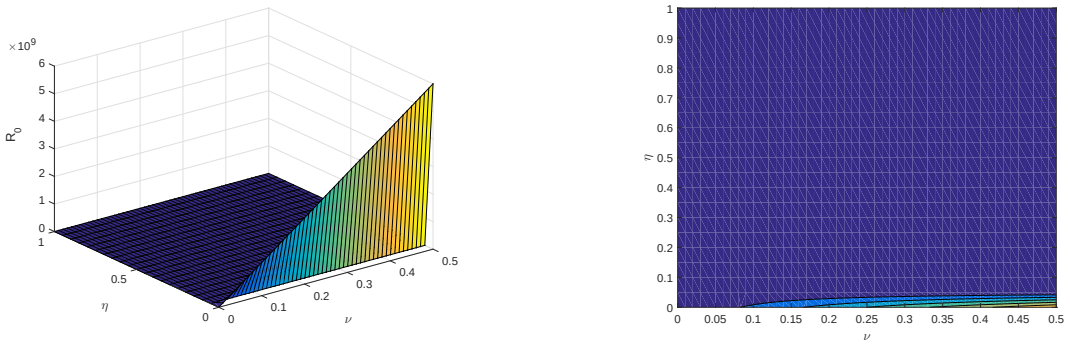

Fig. 10: R_0 and contour phase under parameter ν and η

Figure 12 shows the sensitivity indices of various parameters.

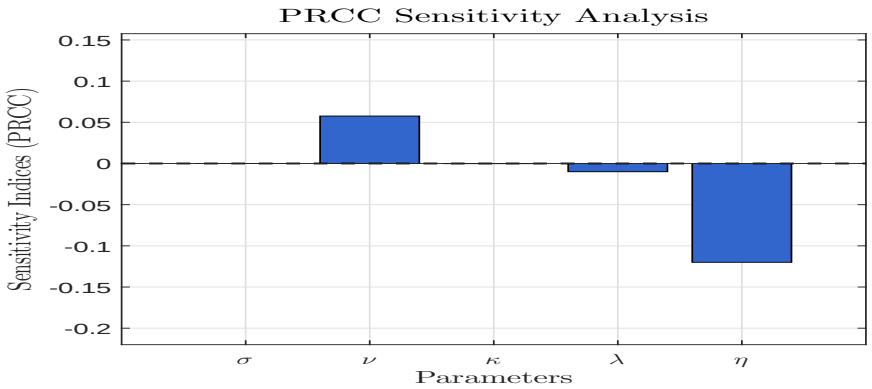

Fig. 12: The bar graph depicts how various parameters influence R_0.

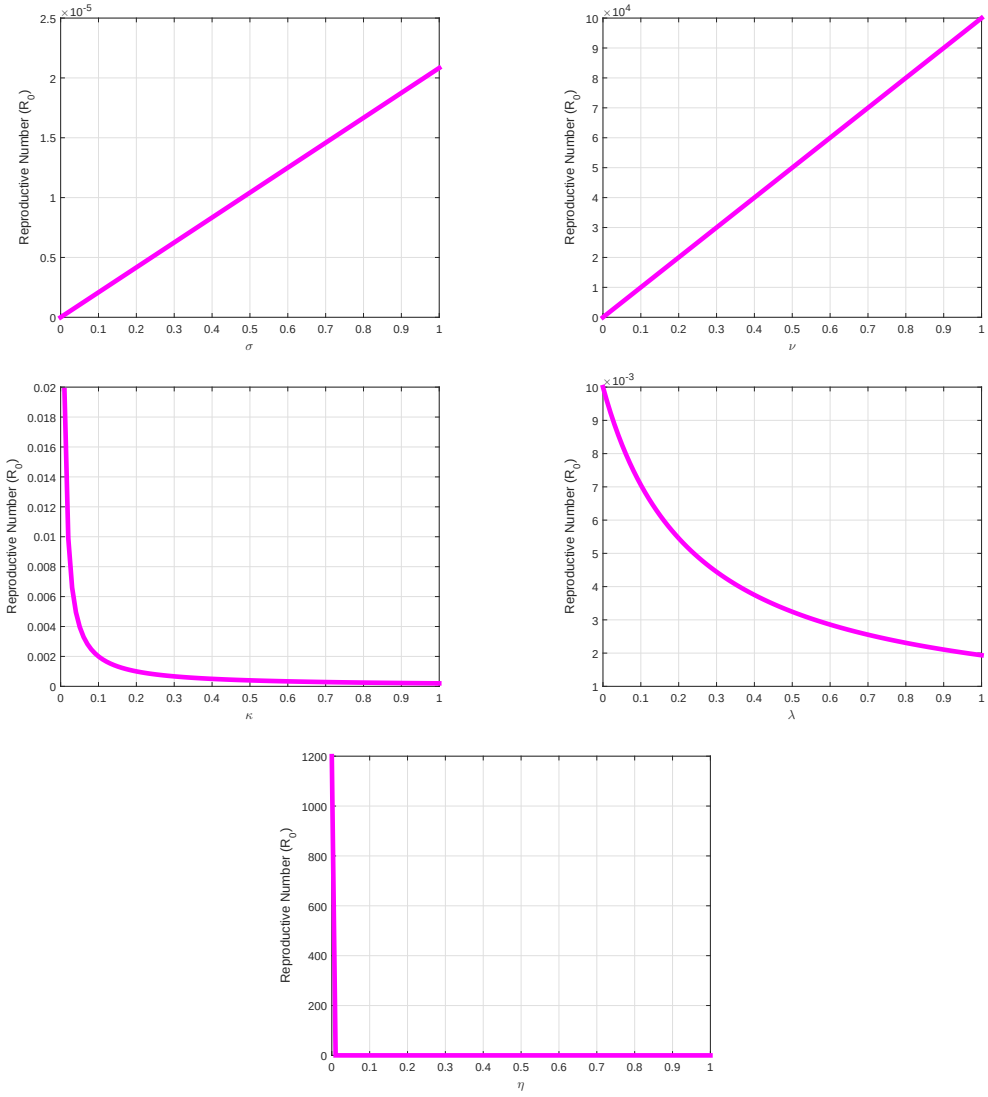

Fig. 11: The graph depicts how various compartmental parameters vary and their influence on R_0

4.1 Local stability analysis of equilibrium points

In our suggested lung cancer scenario, the stable system is said to be resilient and near equilibrium. It courageously reverts to its original configuration and relaxes at equilibrium after minor disruptions. This stabilization or decrease in the general progression of cancer growth is the aim of the local stability analysis. We will be able to define how the patterns of tumor development and the spread of lung cancer at a "population" level work if we are equipped with this idea. This part of the present work deals with a detailed study of the local repelling themselves and fixed points of our lung cancer model associated with tumor-free and endemic states. This section considers stationary solution stable local theories and their proofs. We will develop equations and sketch these graphs.

Theorem 1: When R_0 is less than 1, the disease-free equilibrium point of the proposed lung cancer model is local asymptotically stable; however, when R_0 is more than 1, it becomes unstable.

Proof: In the suggested lung cancer model, the Jacobian matrix at the disease-free equilibrium point D_1 is represented as

follows:

$$J=\begin{pmatrix} \beta-2\beta\gamma T-\delta-\psi C & -\psi T & 0 & 0 & 0 \\ \psi C & \psi T+\nu D-\kappa & \nu C & 0 & 0 \\ 0 & -\nu D & -(\nu C+\eta+\lambda) & 0 & 0 \\ 0 & 0 & \lambda & -d & 0 \end{pmatrix}. \tag{11}$$

Therefore, the characteristic equation can be expressed as:

$$\left|J_0-\Lambda I\right|=0. \tag{12}$$

After evaluating the determinant matrix as described earlier, we derive the following eigenvalues: $\Lambda_1=-a,,\Lambda_2=-d,\Lambda_3=\beta-\delta$, and $\Lambda_4=-\lambda-\eta$. Applying the Routh-Hurwitz criterion confirms that all eigenvalues possess negative real components when $R_0<1$. Hence, the disease-free equilibrium point demonstrates local asymptotic stability.

5 Analyzing Global Stability of the Developed Model

Using a global stability analysis, this section seeks to identify the factors that contribute to the elimination of illness. For this, it uses Lasalle's invariance principle and Lyapunov's method.

Theorem 2: Global asymptotic stability is demonstrated by the lung cancer model's equilibrium when the reproductive number R_0 is greater than 1.

Proof: The Lyapunov's approach can be stated as follows:

$$\begin{aligned}\frac{dL}{dt}&=\left(\frac{T-T^*}{T}\right)(\beta T(1-\gamma T)-\delta T-\psi CT)+\left(\frac{C-C^*}{C}\right)(\psi CT+\nu CD-\kappa C)\\&+\left(\frac{D-D^*}{D}\right)(\sigma-\nu CD-\eta D-\lambda D)+\left(\frac{IL_2-IL_2^*}{IL_2}\right)(\lambda D-dIL_2).\end{aligned} \tag{13}$$

It's essential to note that comprehensively understanding the variations in the function under study requires more than just analyzing its first derivative. To completely understand all the subtleties of these changes, more investigation is required, particularly in the second derivative of the pertinent Lyapunov function of our model.

$$\begin{aligned}\frac{d\dot{L}}{dt}=\ddot{L}&=\frac{d}{dt}\Big\{\sum_{i=1}^{4}\left(1-\frac{M_i^*}{M_i}\right),\\&=\left(\frac{\dot{M}_i}{M_i}\right)^2M_i^*+\left(1-\frac{M_i^*}{M_i}\right)\ddot{M}_i.\end{aligned} \tag{14}$$

Where $M_i=\{T,C,D,IL_2\}$. Herein,

$$\begin{aligned}\ddot{T}&=\beta\dot{T}-2\beta\gamma T\dot{T}-\delta\dot{T}-\psi C\dot{T}-\psi T\dot{C},\\\ddot{C}&=\psi T\dot{C}+\psi C\dot{T}+\nu D\dot{C}+\nu C\dot{D}-\kappa\dot{C},\\\ddot{D}&=-\nu C\dot{D}-\nu D\dot{C}-\eta\dot{D}-\lambda\dot{D},\\I\ddot{L}_2&=\lambda\dot{D}-dI\dot{L}_2.\end{aligned} \tag{15}$$

Subsequently, we obtain the following.

$$\begin{aligned}\frac{d\dot{L}}{dt}=\ddot{L}&=\left(\frac{\dot{T}}{T}\right)^2T^*+\left(\frac{\dot{C}}{C}\right)^2C^*+\left(\frac{\dot{D}}{D}\right)^2D^*+\left(\frac{I\dot{L}_2}{IL_2}\right)^2IL_2^*+\left(1-\frac{T^*}{T}\right)(\beta\dot{T}-2\beta\gamma T\dot{T}-\delta\dot{T}-\psi C\dot{T}-\psi T\dot{C})\\&+\left(1-\frac{C^*}{C}\right)(\psi T\dot{C}+\psi C\dot{T}+\nu D\dot{C}+\nu C\dot{D}-\kappa\dot{C})+\left(1-\frac{D^*}{D}\right)(-\nu C\dot{D}-\nu D\dot{C}-\eta\dot{D}-\lambda\dot{D})\\&+\left(1-\frac{IL_2^*}{IL_2}\right)(\lambda\dot{D}-dI\dot{L}_2)\\\frac{d^2L}{dt^2}&=\prod(T,C,D,IL_2,Z)+\left(1-\frac{T^*}{T}\right)(\beta\dot{T}-2\beta\gamma T\dot{T}-\delta\dot{T}-\psi C\dot{T}-\psi T\dot{C})\\&+\left(1-\frac{C^*}{C}\right)(\psi T\dot{C}+\psi C\dot{T}+\nu D\dot{C}+\nu C\dot{D}-\kappa\dot{C})\\&+\left(1-\frac{D^*}{D}\right)(-\nu C\dot{D}-\nu D\dot{C}-\eta\dot{D}-\lambda\dot{D})+\left(1-\frac{IL_2^*}{IL_2}\right)(\lambda\dot{D}-dI\dot{L}_2).\end{aligned} \tag{16}$$

After substituting the expressions for $\dot{T}$, $\dot{C}$, $\dot{D}$, and $I\dot{L}_2$ from the investigated model and combining them. After simplification, we can express it as follows:
$\frac{d^2L}{dt^2} = \Theta_1 - \Theta_2,$
where

$$\begin{aligned}\Theta_1 &= \prod(T,C,D,IL_2) + \beta^2 T + 2\beta^2\gamma^2 T^3 + 3\beta\gamma\delta T^2 + 2\beta\gamma\psi CT^2 + \delta\psi CT \\ &+ \delta^2 T + \nu\kappa CT + \nu\eta CD + \kappa^2 C + \eta^2 D + \eta\lambda D \\ &+ T^*\left[3\beta^2\gamma T + 2\beta\delta + 2\beta\psi C + \psi^2 CT + \psi\nu CD\right] \\ &+ C^*\left[2\kappa\psi T + \beta\gamma\psi T^2 + \delta\psi T + \psi^2 CT + 2\nu\kappa D + \nu^2 CD + \nu\eta D + \nu\lambda D\right] \\ &+ \frac{D^*}{D}\left(\nu\sigma C + \eta\sigma + \lambda\sigma\right) + D^*\left(\nu\psi CT + \nu^2 CD\right) + \frac{IL_2^*}{IL_2}\left(\nu\lambda CD + \eta\lambda D + \lambda dD\right), \end{aligned} \tag{17}$$

and

$$\begin{aligned}\Theta_2 &= 3\beta^2\gamma T^2 + 2\beta\delta T + \beta\psi CT + 2\psi\kappa CT + \nu\kappa CD + \eta\sigma + T^*\left[\beta^2 + 2\beta^2\gamma^2 T^2 + 3\beta\gamma\delta T\right. \\ &+ \left. 3\beta\gamma\psi CT + 2\delta\psi C + \delta^2 + \psi^2 C^2 + \nu\kappa C\right] + C^*\left[\psi^2 T^2 + 2\psi\nu DT + \beta\psi T + \nu^2 D^2 + \nu\sigma + \kappa^2\right] \\ &+ D^*\left[\nu^2 C^2 + 2\nu\eta C + 2\nu\lambda C + \nu\kappa C + \eta^2 + 2\eta\lambda + \lambda^2\right] + \frac{IL_2^*}{IL_2}\left[\lambda\sigma + d^2 IL_2\right]. \end{aligned} \tag{18}$$

It's apparent that

$$if \quad \Theta_1 > \Theta_2 \quad then \quad \frac{d^2L}{dt^2} > 0, \tag{19}$$

$$if \quad \Theta_1 < \Theta_2 \quad then \quad \frac{d^2L}{dt^2} < 0, \tag{20}$$

$$if \quad \Theta_1 = \Theta_2 \quad then \quad \frac{d^2L}{dt^2} = 0. \tag{21}$$

6 Numerical Solutions

This section is dedicated to validating the proposed numerical scheme through comprehensive numerical evaluations using various methods such as the Euler method, Runge-Kutta method, and the Non-Standard Finite Difference (NSFD) Scheme. The evaluation process encompasses various parametric settings to enrich the strategic environment. Furthermore, we discretize the proposed system (1) for each $N \in \mathbb{N}$ by introducing the set

$$I_N = \{0,1,2,\ldots,N\},$$

over the time interval $T > 0$, which is partitioned into N uniform subintervals of length

$$k = \frac{T}{N}.$$

The corresponding discrete initial conditions are specified as

$$(T_0, C_0, D_0, IL_{20}),$$

where

$$T^0 = T_0, \quad C^0 = C_0, \quad D^0 = D_0, \quad IL_2^0 = IL_{20}.$$

Euler Method

In this section, we outline a numerical scheme utilizing the Euler method to numerically solve the system (1) as follows:

$$\begin{aligned} T^{m+1} &= T^m + h\left[\beta T^m(1-\gamma T^m) - \delta T^m - \psi C^m T^m\right], \\ C^{m+1} &= C^m + h[\psi C^m T^m + \nu C^m D^m - \kappa C^m], \\ D^{m+1} &= D^m + h[\sigma - \nu C^m D^m - \eta D^m - \lambda D^m], \\ IL_2^{m+1} &= IL_2^m + h[\lambda D^m - d IL_2^m], \end{aligned} \tag{22}$$

where "h" denotes the discretization interval in this context.

Runge−Kutta method

The Runge-Kutta method is posited in epidemiological modeling as a deliberate method to address the concerns of complex differential equations that govern the disease spread. RK method of fourth order noted its accuracy, enables the correct acquisition of the result of a mathematical problem, and is easy to adopt for different types of mathematical problems. This is the ability to use the techniques of transmission, and intervention is the main benefit of such an approach, leading, therefore, to a valuable understanding of the transmission speed and dynamics of the disease. The model we have chosen would have been immeasurable with RK-4, which has made it possible for us to attain more complex results from our simulations. Therefore, the aforementioned design for the system (1) is described below.

Stage 1:

$$\begin{aligned}
K_1 &= h[\beta T^m(1-\gamma T^m) - \delta T^m - \psi C^m T^m],\\
L_1 &= h[\psi C^m T^m + \nu C^m D^m - \kappa C^m],\\
M_1 &= h[\sigma - \nu C^m D^m - \eta D^m - \lambda D^m],\\
N_1 &= h[\lambda D^m - d IL_2^m],
\end{aligned} \tag{23}$$

Stage 2:

$$K_2 = h\left[\beta\left(T^m+\frac{K_1}{2}\right)(1-\gamma\left(T^m+\frac{K_1}{2}\right)) - \delta\left(T^m+\frac{K_1}{2}\right) - \psi\left(C^m+\frac{L_1}{2}\right)\left(T^m+\frac{K_1}{2}\right)\right], \tag{24}$$

$$L_2 = h\left[\psi\left(C^m+\frac{L_1}{2}\right)\left(T^m+\frac{K_1}{2}\right) + \nu\left(C^m+\frac{L_1}{2}\right)\left(D^m+\frac{M_1}{2}\right) - \kappa\left(C^m+\frac{L_1}{2}\right)\right], \tag{25}$$

$$M_2 = h\left[\sigma - \nu\psi\left(C^m+\frac{L_1}{2}\right)\left(D^m+\frac{M_1}{2}\right) - \eta\left(D^m+\frac{M_1}{2}\right) - \lambda\left(D^m+\frac{M_1}{2}\right)\right], \tag{26}$$

$$N_2 = h\left[\lambda\left(D^m+\frac{M_1}{2}\right) - d\left(IL_2^m+\frac{N_1}{2}\right)\right], \tag{27}$$

Stage 3:

$$K_3 = h\left[\beta\left(T^m+\frac{K_2}{2}\right)(1-\gamma\left(T^m+\frac{K_2}{2}\right)) - \delta\left(T^m+\frac{K_2}{2}\right) - \psi\left(C^m+\frac{L_2}{2}\right)\left(T^m+\frac{K_2}{2}\right)\right], \tag{28}$$

$$L_3 = h\left[\psi\left(C^m+\frac{L_2}{2}\right)\left(T^m+\frac{K_2}{2}\right) + \nu\left(C^m+\frac{L_2}{2}\right)\left(D^m+\frac{M_2}{2}\right) - \kappa\left(C^m+\frac{L_2}{2}\right)\right], \tag{29}$$

$$M_3 = h\left[\sigma - \nu\psi\left(C^m+\frac{L_2}{2}\right)\left(D^m+\frac{M_2}{2}\right) - \eta\left(D^m+\frac{M_2}{2}\right) - \lambda\left(D^m+\frac{M_2}{2}\right)\right], \tag{30}$$

$$N_3 = h\left[\lambda\left(D^m+\frac{M_2}{2}\right) - d\left(IL_2^m+\frac{N_2}{2}\right)\right], \tag{31}$$

Stage 4:

$$K_4 = h\left[\beta\left(T^m+K_1\right)(1-\gamma(T^m+K_1)) - \delta\left(T^m+K_1\right) - \psi\left(C^m+L_1\right)\left(T^m+K_1\right)\right], \tag{32}$$

$$L_4 = h\left[\psi\left(C^m+L_1\right)\left(T^m+K_1\right) + \nu\left(C^m+L_1\right)\left(D^m+M_1\right) - \kappa\left(C^m+L_1\right)\right], \tag{33}$$

$$M_4 = h\left[\sigma - \nu\left(C^m+L_1\right)\left(D^m+M_1\right) - \eta\left(D^m+M_1\right) - \lambda\left(D^m+M_1\right)\right], \tag{34}$$

$$N_4 = h\left[\lambda\left(D^m+M_1\right) - d\left(IL_2^m+N_1\right)\right], \tag{35}$$

Finally, we derive the generalized formulation of the proposed system.

$$T^{m+1} = T^m + \frac{1}{6}\left[K_1 + 2(K_2+K_3) + K_4\right], \tag{36}$$

where, $m = 0, 1, 2, ...$

Non-Standard Finite Difference (NSFD) Scheme

In this section, we construct a nonstandard finite difference (NSFD) scheme that reproduces the dynamics of the continuous model given in system (1) [29]. Following the approach of Anguelov and Lubuma (2001), we denote

$$Y_k = \left(T_k, C_k, D_k, IL_{2,k}\right)^T$$

as the discrete approximation of $X(t_k)$, where $t_k = k\Delta t$ for $k \in \mathbb{N}$, and $h = \Delta t > 0$ denotes the time step. Then,

$$\begin{aligned}
\frac{T^{k+1}-T^k}{\vartheta} &= \beta T^k - \beta\gamma T^k T^{k+1} - \psi C^k T^{k+1},\\
\frac{C^{k+1}-C^k}{\vartheta} &= \psi C^k T^{k+1} + \nu C^k D^k - \kappa C^{k+1},\\
\frac{D^{k+1}-D^k}{\vartheta} &= \sigma - \nu C^{k+1} D^{k+1} - \eta D^{k+1} - \lambda D^{k+1},\\
\frac{IL_2^{k+1}-IL_2^k}{\vartheta} &= \lambda D^{k+1} - dIL_2^{k+1},
\end{aligned} \tag{37}$$

where

$$\vartheta = \vartheta(h) = \frac{1-e^{-(\eta+\lambda)h}}{\eta+\lambda}. \tag{38}$$

The discrete approach (37) adheres to Mickens' criteria, making it an NSFD scheme (Mickens, 1994) [30] and is formulated as described in (Anguelov and Lubuma, 2001) [29].

Rule 1: Equation (38) ensures an asymptotic link by substituting the normal denominator $h = \Delta t$ of discrete derivatives for the complex denominator function. This is represented by $\vartheta(h) = h + O(h^2)$.

The inclusion of parameters η and λ aims to enhance the functionality of the denominator function ϑ, aligning it more closely with the continuous model's dynamics. Gumel (2014) [31,32] and Lubuma and Patidar (2007) explore the importance of such complex denominator functions in precise approaches applicable to a variety of dynamical systems.

Rule 2: Expressions like $C(t_k), T(t_k), \approx, C_{k+1}, T_k$ instead of $C(t_k), T(t_k), \approx, C_k, T_k$, and $C(t_k), D(t_k), \approx, C_{k+1}, D_k$ instead of $C(t_k), D(t_k), \approx, C_k, D_k$ instead of $C(t_k), D(t_k), \approx, C_k, D(t_k), D(t_k), \approx, C_k, D_k$.

6.1 Analysis of the Numerical scheme

Theorem 3: Consider the dynamical system described by equation (1), representing the continuous model. On the biologically feasible domain η, the system can be equivalently formulated as the NSFD scheme (37).

Proof: We begin by proving the positivity of the scheme (2-5). Subsequently, we show that the NSFD scheme (2-5) can be explicitly formulated.

$$\begin{aligned}
T^{k+1} &= \frac{\vartheta\left(\beta T^k - \beta\gamma T^k T^{k+1}\right) + T^k}{1+\vartheta(\delta+\psi C^k)},\\
C^{k+1} &= \frac{\vartheta\left(\psi C^k A^* + \nu C^k D^k\right) + C^k}{1+\vartheta\kappa},\\
D^{k+1} &= \frac{\vartheta\sigma + D^k}{1+\vartheta(\nu B^* + \eta + \lambda)},\\
IL_2^{k+1} &= \frac{\vartheta\lambda C^* + IL_2^k}{1+\vartheta d}.
\end{aligned} \tag{39}$$

Where
$A^* = \frac{\vartheta\left(\beta T^k - \beta\gamma T^k T^{k+1}\right)+T^k}{1+\vartheta(\delta+\psi C^k)}$, $B^* = \frac{\vartheta\left(\psi C^k A^* + \nu C^k D^k\right)+C^k}{1+\vartheta\kappa}$, $C^* = \frac{\vartheta\sigma+D^k}{1+\vartheta(\nu B^*+\eta+\lambda)}$ and $D^* = \frac{\vartheta\lambda C^*+IL_2^k}{1+\vartheta d}$.

Consequently, if the discrete variables in the previous iteration were non-negative, then $T^{k+1} \geq 0$, $C^{k+1} \geq 0$, $D^{k+1} \geq 0$, and $IL_2^{k+1} \geq 0$. It is essential to prove the positive invariance of η. Summing up equations (4) and (5) yields:

$$\begin{aligned}
(1+d\vartheta)M_{k+1} &= \vartheta\sigma + M_k - \vartheta(\nu C^{k+1} + \eta)D^{k+1} \leq \vartheta\sigma + M_k,\\
(1+d\vartheta)M_{k+1} &\leq \vartheta\sigma + M_k.
\end{aligned} \tag{40}$$

Therefore $M_{k+1} \leq \frac{\vartheta\sigma}{1+d\vartheta}$ whenever $M_k \leq \frac{\vartheta\sigma}{1+d\vartheta}$.

The a priori bounds for IL_2k+1 and C_{k+1} are easily established as they are both less than or equal to M_{k+1}. The evidence is now complete.

7 Discussion on Simulation Results

This part delves into the analysis of our suggested model, highlighting the dynamic interactions between model parameters and their combined impact on the dynamics of lung cancer transmission in society. We use sophisticated methodologies to perform numerical simulations to acquire theoretical conclusions and explore the efficacy of the previously established analytical results.

The recently created system, called TCDIL_2, is fully examined through simulation. Using various methods in the lung cancer model, we have come to some interesting conclusions. Graphical representations of each compartment of the developed model, $T(t)$, $C(t)$, $D(t)$, and $IL_2(t)$, are shown in Figures 13, 14, 15 and 16. These representations compare and display the simulation results achieved using the suggested numerical approaches. These findings offer a trustworthy solution made possible by the NSFD techniques used. The study's reliability is ensured by using MATLAB to calculate the approximate answers in simulation form. $\gamma = 0.00000000102$, $\beta = 0.0514$, $\psi = 0.0000001$, $\kappa = 0.02$, $\delta = 0.1$, $\nu = 0.00000001$, $\sigma = 480$, $\lambda = 0.0000002$, $\eta = 0.24$, $a = 0.04$ and $d = 0.0003$ are the parametric values that were utilized.

Figures 13 and 14 depict the dynamics of tumor cells (T) and $CD8+T$ cells (C), respectively. In each compartment, there is a notable decline followed by stabilization over time. Figures 15 and 16 show the variations in the populations of dendritic cells (D) and cytokines (IL_2), respectively. In both cases, the population sharply increases before stabilizing, observed using RK4 and NSFD but not Euler's method. We observe a significant reduction in cancer cell numbers due to the presence of anticancer cells and anti-PD-L1 agents, as shown in Figures 14b, 14c, and 16b, 16c. NSFD demonstrates unconditional convergence, while Euler's and RK4 struggle with large step sizes. Figures 13a and 14a illustrate Euler's method leading to divergence with increased step size. Although RK4 generally performs better, it also diverges for larger steps. This comparison highlights the necessity for more efficient approaches in combating cancer cell transmission within the body. Exploring different methods allows us to achieve reliable results across all compartments, drawing insights from steady-state analysis and varying step sizes.

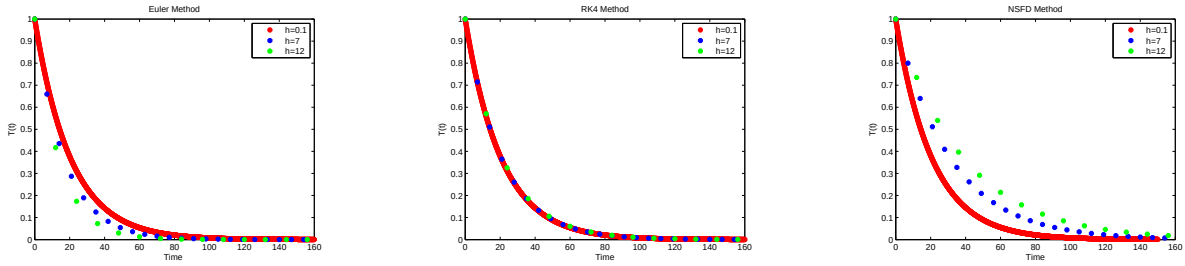

(a) (a). Euler (b) (b). RK4 (c) (c). NSFD

Fig. 13: Simulating $T(t)$ through Various Techniques

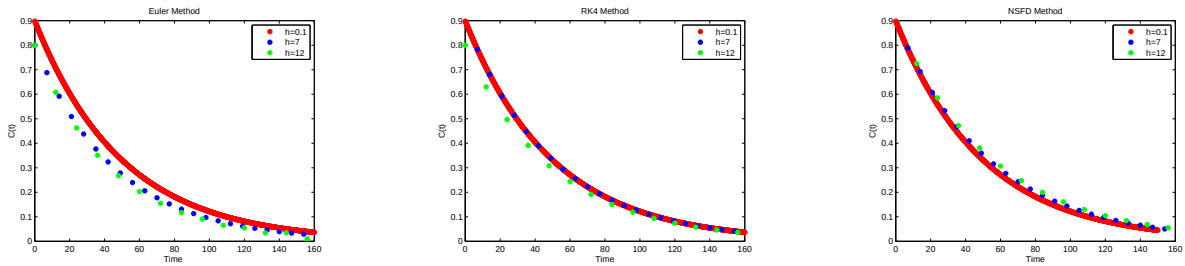

(a) (a). Euler (b) (b). RK4 (c) (c). NSFD

Fig. 14: Simulating $C(t)$ through Various Techniques

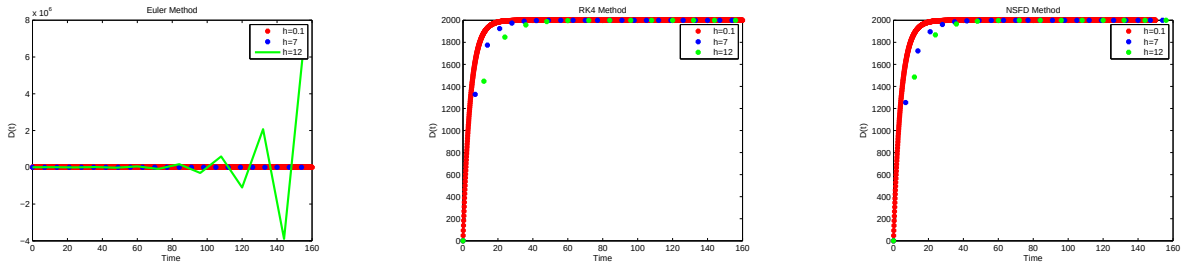

(a) (a). Euler (b) (b). RK4 (c) (c). NSFD

Fig. 15: Simulating $D(t)$ through Various Techniques

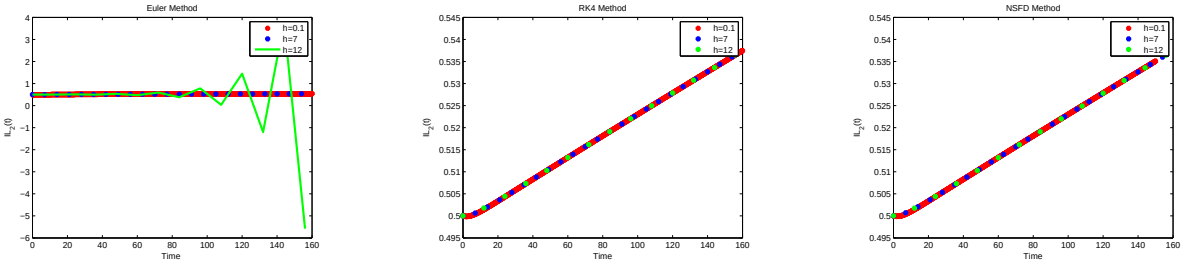

(a) (a). Euler (b) (b). RK4 (c) (c). NSFD

Fig. 16: Simulating $IL_2(t)$ through Various Techniques

8 Conclusion

Mathematical formulations play a crucial role in understanding disease dynamics within communities. This study introduces a novel deterministic mathematical TCDIL_2 model for lung cancer, integrating cytokine IL_2 across four epidemiological compartments. We aim to propose effective disease control strategies by leveraging anti-cancer cells to boost individual's immune responses and foster a disease-free environment. Emphasizing the criticality of early detection and treatment in lung cancer, we assess the model's stability through comprehensive quantitative and qualitative analysis within a continuous dynamical system, ensuring its broad applicability across various parameter settings. Calculating the fundamental reproduction number (R_0), locating endemic equilibrium sites, and assessing stability features by the accepted theory are all part of the validation process. A critical statistic for forecasting disease propagation rates and possible outbreaks is R_0. While sensitivity analysis looks at how parameter changes affect the spread of illness, local stability analysis sheds light on the dynamics of epidemics under limited settings.

Further, worldwide strategies to stop the spread of lung cancer are investigated, with particular attention to how IL_2 affect immunodeficient people. The global stability analysis is performed using the Lyapunov direct approach, while numerical solutions are found using the Non-Standard Finite Difference (NSFD) scheme. Applying IL_2 cytokine measures aids in our understanding of the dynamics of lung cancer control in the community. Using MATLAB for simulations, we verify the dependability of these results by comparing them with Euler's and RK4 approaches. Our models' insights into post-intervention lung cancer control will benefit future forecasts and outbreak management. Sensitivity analysis probes parameter variations' effects on disease transmission.

Extending the developed model to incorporate a fractional order approach while retaining optimal control promises intriguing insights in future endeavours. The fractional order scheme's capacity to utilize available data will enhance our understanding of disease transmission dynamics. Furthermore, we will thoroughly investigate the suitability of the suggested plan for a range of data sets that include different geographic regions, socioeconomic classes common in society, and different levels of access to medical services.

Data availability statement

The data supporting this study's findings are available within the article.

Conflict of interest

None declared.

Acknowledgments

This study is supported via funding from Prince Sattam bin Abdulaziz University project number (PSAU/2024/R/1445)

References

[1] C. S. Chou, A. Friedman, *Introduction to mathematical biology*, Springer undergraduate texts in mathematics and technology, Springer International Publishing, **1**(2016), 1-10, (2016).
[2] E. K. Yeargers, R. W. Shonkwiler, J. V. Herod, *An introduction to the mathematics of biology: With computer algebra models-Chapter 1: Biology, mathematics, and a mathematical biology laboratory*, Springer Science and Business Media, pp. 1-8, (2013).
[3] Maheswaran, Harshyini,et all, Cytotoxic study of zinc oxide nanoparticles on cervical cancer cell line, *Journal of Experimental Biology and Agricultural Sciences,*, **11(5)**(2023), 815-821, (2023). https://doi.org/10.18006/2023.11(5).815.821.
[4] N. Bellomo, A. Bellouquid, M. Delitala, Mathematical topics on the modeling of multicellular systems in competition between tumor and immune cells, *Mathematical Models and Methods in Applied Sciences*, 1683-1733, (2004).
[5] T. Roose, S. J. Chapman, P. K. Maini, Mathematical models of avascular tumor growth, *SIAM Review* , **49**(2007), 179-208, (2007). https://doi.org/10.1137/S0036144504446291.
[6] N. Bellomo, L. Preziosi, Modelling and mathematical problems related to tumor evolution and its interactions with the immune system, *Mathematical and Computer Modelling*, **32**(2000), 413-452, (2000). https://doi.org/10.1016/S0895-7177(00)00143-6.
[7] H. M. Byrne, T. Alarcon, M. R. Owen, S. D. Webb, P. K. Maini, Modeling aspects of cancer dynamics: A review, *Philosophical Transactions of the Royal Society A*, **364**(2006), 1563-1578, (2006).
[8] F. Castiglione, B. Piccoli, Cancer immunotherapy, mathematical modeling and optimal control, *Journal of Theoretical Biology*, **247**(2007), 723-732, (2007).
[9] S. Abdal, M. F. Tabassumb, and A. Shahzad, Hybrid Fractional Operator for Epidemic Model analysis and application, *ournal of Mathematical Modeling and Fractional Calculus*, **1**(1), 25-37, (2024).
[10] A. Hussain, M. Hammad, A. A. Rahimzai, W. S. Koh, and I. Khan, Dynamical analysis and soliton solutions of the space-time fractional Kaup-Boussinesq system. *Partial Differential Equations in Applied Mathematics*, 101205, (2025).
[11] H. Khan, W. F. Alfwzan, J. Alzabut, D. K. Almutairi, M. A. Azim, and R. Thinakaran, Artificial Intelligence And Neural Networking For An Analysis Of Fractal-Fractional Zika Virus Model, *FRACTALS (fractals)*, **33**(08), 1-18, (2025).
[12] K. Faiz, A. Ahmad, M. S. Khan, and S. Abbas, Control of Marburg Virus Disease Spread in Humans under Hypersensitive Response through Fractal-Fractional, *Journal of Mathematical Modeling and Fractional Calculus*, **1**(1), 88-113, (2024).
[13] L. G. de Pillis, A. E. Radunskaya, and C. L. Wiseman, A validated mathematical model of cell-mediated immune response to tumor growth, *American Association for Cancer Research*, **65**(17), 7950-7958, (2005).
[14] T. Trisilowati, S. McCue, and D. Mallet, Numerical solution of an optimal control model of dendritic cell treatment of a growing tumour, *ANZIAM Journal*, **54**(2012), 664-680, (2012).
[15] P. Unni and P. Seshaiyer, Mathematical modeling, analysis, and simulation of tumor dynamics with drug interventions, *Computational and Mathematical Methods in Medicine*, 2019, Article ID 4079298, 13 pages, (2019).
[16] D. Kirschner and A. Tsygvintsev, On the global dynamics of a model for tumor immunotherapy, *Mathematical Biosciences and Engineering*, **6**(3), 573-583, (2009).
[17] D. Kirschner and J. C. Panetta, Modeling immunotherapy of the tumor - immune interaction, *Journal of Mathematical Biology*, **37**(3), 235-252, (1998).
[18] W. K. Decker, R. F. da Silva, M. H. Sanabria et al., Cancer immunotherapy: historical perspective of a clinical revolution and emerging preclinical animal models, *Frontiers in Immunology*, **8**, 829, (2017).
[19] A. Waldman, J. Fritz, and M. Lenardo, A guide to cancer immunotherapy: from T cell basic science to clinical practice, *Nature Reviews Immunology*, **20**(11), 651-668, (2020).
[20] K. J. Hiam-Galvez, B. M. Allen, and M. H. Spitzer, Systemic immunity in cancer, *Nature Reviews. Cancer*, **21**(6), 345-359, (2021).
[21] A. S. Kartono, "Mathematical modeling of the effect of boosting tumor infiltrating lymphocyte in immunotherapy, *Pakistan Journal of Biological Sciences*, **16**(20), 1095-1103, (2013).
[22] L. M. McLane, M. S. Abdel-Hakeem, and E. J. Wherry, CD8 T cell exhaustion during chronic viral infection and cancer, *Annual Review of Immunology*, **37**(1), 457-495, (2019).

[23] M. Philip and A. Schietinger, CD8+ T cell differentiation and dysfunction in cancer, *Nature Reviews. Immunology*, **22**(4), 209-223, (2022).
[24] M. Casiraghi, G. Sedda, E. Del Signore et al., Surgery for small cell lung cancer: when and how, *Lung Cancer*, **152**, 71-77, (2021).
[25] M. Liang, M. Chen, S. Singh, and S. Singh, Prognostic nomogram for overall survival in small cell lung cancer patients treated with chemotherapy: a SEER-based retrospective cohort study, *Advances in Therapy*, **39**(1), 346-359, (2022).
[26] C. Chao, D. Di, M. Wang, Y. Liu, B. Wang, and Y. Qian, Identifying octogenarians with non-small cell lung cancer who could benefit from surgery: a population-based predictive model,"*Frontiers in Surgery*, **9**, 1-13, (2022).
[27] H. S. Li, J. L. Li, X. Yan, H. Y. Xu, L. Q. Zhou, X. S. Hu, and Y. Wang, Efficacy of dacomitinib in patients with non-small cell lung cancer carrying complex EGFR mutations: a real-world study. Journal of Thoracic Disease, **14**(5), 1428-1440, (2022).
[28] M. A. Ullah, and U. K. Mallick, Mathematical Modeling and Analysis on the Effects of Surgery and Chemotherapy on Lung Cancer, *Journal of Applied Mathematics*, **23**, 1-16, (2023).
[29] R. Anguelov and J. M. S. Lubuma, Contributions to the mathematics of the nonstandard finite difference method and applications, *Numerical Methods for Partial Differential Equations*, **17**(5), 518-543, (2001).
[30] R. E. Mickens, *Nonstandard finite difference models of differential equations*, World Scientific, Singapore, (1994).
[31] J. M. S. Lubuma and K. C. Patidar, Non-standard methods for singularly perturbed problems possessing oscillatory/layer solutions, *Applied Mathematics and Computation*, **187**(2), 1147-1160, (2007).
[32] A. Gumel, *Mathematics of Continuous and Discrete Dynamical Systems*, Vol. 618, American Mathematical Society, Providence, Rhode Island, (2014).
[33] M. Farman, A. Ahmad, A. Akgül, M. U. Saleem, K. S. Nisar, and V. Vijayakumar, Dynamical behavior of tumor-immune system with fractal-fractional operator. AIMS Mathematics, **7**(5), 8751-8773, (2022).
[34] M. Farman, M. U. Saleem, M. O. Ahmed, and A. Ahmad, Stability analysis and control of the glucose insulin glucagon system in humans, *Chinese Journal of Physics*, **56**(4), 1362-1369, (2018).
[35] A. Ahmad, M. O. Kulachi, M. Farman, M. U. D. Junjua, M. Bilal Riaz, and S. Riaz, Mathematical modeling and control of lung cancer with IL 2 cytokine and anti-PD-L1 inhibitor effects for low immune individuals, *Plos one*, **19**(3), e0299560, (2024).
[36] K. S. Nisar, M. O. Kulachi, A. Ahmad, M. Farman, M. Saqib, and M. U. Saleem, Fractional order cancer model infection in human with CD8+ T cells and anti-PD-L1 therapy: simulations and control strategy, *Scientific Reports*, **14**(1), 16257, (2024).
[37] A. R. Seadawy, M. Arshad, and D. Lu, The weakly nonlinear wave propagation theory for the Kelvin-Helmholtz instability in magnetohydrodynamics flows. *Chaos, Solitons & Fractals*, **139**, 110141, (2020).
[38] N. Nasreen, M. N. Rafiq, U. Younas, M. Arshad, M. Abbas, and M. R. Ali, Stability analysis and dynamics of solitary wave solutions of the (3+ 1)-dimensional generalized shallow water wave equation using the Ricatti equation mapping method, *Results in Physics*, **56**, 107226, (2024).
[39] M. A. Umer, M. Arshad, A. R. Seadawy, I. Ahmed, and M. Tanveer, Exploration conversations laws, different rational solitons and vibrant type breather wave solutions of the modify unstable nonlinear Schrödinger equation with stability and its multidisciplinary applications, *Optical and Quantum Electronics*, **56**(3), 420, (2024).
[40] M. Arshad, A. R. Seadawy, Tanveer, and F. Yasin, Study on abundant dust-ion-acoustic solitary wave solutions of a (3+ 1)-dimensional extended Zakharov-Kuznetsov dynamical model in a magnetized plasma and its linear stability, *Fractal and Fractional*, **7**(9), 691, (2023).
[41] M. Arshad, S. F. Aldosary, S. Batool, I. Hussain, N. Hussain, Exploring fractional-order new coupled Korteweg-de Vries system via improved Adomian decomposition method. *Plos one*, **19**(5), e0303426, (2024).